Published in final edited form as:
Cell Signal. 2010 October ; 22(10): 1543–1553. doi:10.1016/j.cellsig.2010.05.023.

(*S*)-FTY720-Vinylphosphonate, an Analogue of the Immunosuppressive Agent FTY720, Is a Pan-antagonist of Sphingosine 1-Phosphate GPCR Signaling and Inhibits Autotaxin Activity

William J. Valentine[1,*], **Gyöngyi N. Kiss**[1,*], **Jianxiong Liu**[1], **E Shuyu**[1], **Mari Gotoh**[1,2], **Kimiko Murokami-Murofushi**[2], **Truc Chi Pham**[3], **Daniel L. Baker**[3], **Abby L. Parrill**[3], **Xuequan Lu**[4], **Chaode Sun**[4], **Robert Bittman**[4], **Nigel J. Pyne**[5], and **Gabor Tigyi**[1,#]

[1]Department of Physiology, University of Tennessee Health Science Center, Memphis, Tennessee 38163 USA

[2]Department of Biology, Ochanomizu University, Tokyo, Japan

[3]Computational Research on Materials Institute, Department of Chemistry, University of Memphis, Memphis, TN 38152 USA

[4]Department of Chemistry and Biochemistry, Queens College of The City University of New York, Flushing, New York 11367-1597 USA

[5]Cell Biology Group, Strathclyde Institute of Pharmacy and Biomedical Sciences, University of Strathclyde, 27 Taylor St, Glasgow, G4 0NR, UK

Abstract

FTY720 (Fingolimod™), a synthetic analogue of sphingosine 1-phosphate (S1P), activates four of the five EDG-family S1P receptors and is in a phase-III clinical study for the treatment of multiple sclerosis. (*S*)-FTY720-phosphate (FTY720-P) causes $S1P_1$ receptor internalization and targeting to the proteasomal degradative pathway, and thus acts as a functional antagonist of $S1P_1$ by depleting the functional $S1P_1$ receptor from the plasma membrane. Here we describe the pharmacological characterization of two unsaturated phosphonate enantiomers of FTY720, (*R*)- and (*S*)-FTY720-vinylphosphonate. (*R*)-FTY720-vinylphosphonate was a full agonist of $S1P_1$ (EC_{50} 20 ± 3 nM). In contrast, the (*S*) enantiomer failed to activate any of the five S1P GPCRs and was a full antagonist of $S1P_{1,3,4}$ (K_i 384 nM, 39 nM, and 1190 nM, respectively) and a partial antagonist of $S1P_2$, and $S1P_5$. Both enantiomers dose-dependently inhibited lysophospholipase D (recombinant autotaxin) with K_i values in the low micromolar range, although with different enzyme kinetic mechanisms. When injected into mice, both enantiomers caused transient peripheral lymphopenia. (*R*)- and (*S*)-FTY720-vinylphosphonates activated ERK1/2, AKT, and exerted an antiapoptotic effect in camptothecin-treated IEC-6 intestinal epithelial cells, which primarily express $S1P_2$ transcripts and traces of $S1P_5$. (*S*)-FTY720-vinylphosphonate is the first pan-antagonist of S1P receptors and offers utility in probing S1P responses in vitro and in vivo.

[#] To whom correspondence should be addressed: gtigyi@uthsc.edu Phone: (901) 448-4793. Fax: (901) 448-7126.
[*]Contributed equally

The biological effects of the (*R*)- and (*S*)-FTY720-vinylphosphonate analogues underscore the complexity of FTY720 cellular targets.

Keywords

FTY720; sphingosine 1-phosphate; lysophosphatidic acid; autotaxin; lysophospholipase D; lymphocyte egress; EDG receptor; inhibitor

1. Introduction

FTY720 (2-amino-[2-(4-*n*-octylphenyl)ethyl]-1,3-propanediol, Figure 1) is a synthetic analogue of the well-known chiral sphingolipid myriocin and is now in phase 3 clinical trials for the treatment of multiple sclerosis under the trade name Fingolimod [1]. FTY720 is phosphorylated in vivo by sphingosine kinase 2 to become the active drug metabolite (*S*)-FTY720-phosphate (FTY720-P). FTY720-P is an agonist at nanomolar concentrations for four of the five Endothelial Differentiation Gene (EDG)-family S1P receptors, $S1P_{1,3,4,\&5}$. FTY720-P inhibits the egress of lymphocytes from lymphoid tissues and exerts a potent immunosuppressive action by causing the sequestration and apoptosis of lymphocytes in secondary lymphoid organs [2]. This action is mediated through downregulating cell surface expression of the $S1P_1$ receptor. FTY720-P is a functional antagonist of $S1P_1$ in that it activates this receptor, causing its internalization and subsequent polyubiquitination leading to proteasomal degradation of $S1P_1$, which in turn renders lymphocytes unresponsive to S1P [3] Furthermore, FTY720 inhibits multiple enzymes including sphingosine 1-phosphate (S1P) lyase and sphingosine kinase 1 [4], phospholipase A_2 [5], as well as ceramide synthase [6,7]. FTY720-P inhibits lysophospholipase D/autotaxin (ATX) [8], which generates lysophosphatidic acid (LPA) from lysophosphatidylcholine and also S1P from sphingosylphorphorylcholine. FTY720 has been shown to activate PP2A-like phosphatases [9,10] .

The unique immunosuppressive action of FTY720-P has generated considerable interest in developing $S1P_1$ antagonists and analogues of FTY720 for applications in a wide range of diseases ranging from autoimmune disorders to cancer. We recently reported [11] the first asymmetric synthesis of the chiral phosphonate and vinylphosphonate analogues of FTY720 (Fig. 1). Here we provide a comprehensive pharmacological and biological characterization of these chiral FTY720-phosphonates and FTY720-vinylphosphonates, as well as their enantiomer-specific pharmacological actions. Unlike FTY720-P, (*S*)-FTY720-vinylphosphonate (referred to here as (*S*)-ene) did not activate any of the five S1P receptors of the EDG family of GPCR, nor did it activate P2Y10, a putative dual specificity LPA and S1P receptor. In contrast, (*R*)-FTY720-vinylphosphonate (*R*)-ene) was a full agonist of $S1P_1$. (*S*)-ene was found to inhibit all five EDG-family S1P receptors in a dose-dependent manner. When injected into mice, both (*R*)- and (*S*)-ene caused transient lymphopenia. (*S*)-ene and (*R*)-ene activated ERK1/2 and AKT kinases, and inhibited DNA damage-induced apoptosis elicited by campthothecin in IEC-6 epithelial cells. The two chiral vinylphosphonates inhibited ATX, but acted by different enzyme kinetic mechanisms. Thus (*R*)- and (*S*)-FTY720-vinylphosphonates are novel enantioselective agents with significant potential utility in probing the molecular targets of FTY720 and S1P.

2. Materials and Methods

2.1. Materials

Lysophosphatidic acid (18:1) and S1P were purchased from Avanti Polar Lipids (Alabaster, AL). (*S*)-FTY720-phosphate (referred to here as FTY720-P) was provided by Novartis. The

R and *S* enantiomers of FTY720-phosphonate and FTY720-vinylphosphonate were prepared as described previously [11]. For calcium mobilization assays, LPA, S1P, FTY720-P, and the *R* and *S* enantiomers of FTY720 phosphonate and vinylphosphonate were prepared as 1 mM stock solutions in phosphate-buffered saline (PBS) in an equimolar complex with charcoal-stripped, fatty acid free bovine serum albumin (BSA; Sigma, St. Louis, MO). Pertussis toxin (PTX) was purchased from Biomol Laboratories (Plymouth Meeting, PA). The fluorescent ATX substrate FS-3 was purchased from Echelon Biosciences (Salt Lake City, UT).

2.2. Cell culture and transfection

HTC4 cells stably transfected with $S1P_{1-4}$ or the control vector pCDEF3 containing the Geneticin–resistance gene were a generous gift of Dr. Edward Goetzl (University of California, San Francisco) [12]. For transient expression of $S1P_5$, 3.5×10^6 HTC4 cells were seeded onto 10-cm dishes. After 12 h, the cells were cotransfected with $S1P_5$ in pCR3.1 vector and $G\alpha_{qz5}$ in pcDNA-1 (a gift of Dr. Bruce Conklin, University of California, San Francisco) using Effectene Transfection Reagent (Qiagen, Valencia, CA) according to the manufacturer's instructions. We used a 3:1 ratio of $S1P_5$ to Ga_{qz5} in our transfections in order to minimize a slight endogenous Ca^{2+} response to S1P detected when the cells were transfected with Ga_{qz5} alone. Cells were incubated with transfection complexes overnight and then replated into 96-well microplates for use in receptor activation assays. CHO cells stably expressing P2Y10 fused to Gα16 (a gift of Dr. Norihisa Fujita, Ritsumeikan University, Kusatsu Shiga, Japan) were maintained in HAM's F12 medium supplemented with 10% (v/v) fetal bovine serum, 100 units/mL penicillin, 10 μg/mL streptomycin, and 2 mM glutamine. HEK293 cells were maintained in Dulbecco's modified Eagle medium supplemented with 10% (v/v) fetal bovine serum, 100 units/mL penicillin, 10 μg/mL streptomycin, and 2 mM glutamine, and were transfected with a $S1P_1$ construct containing eGFP fused to the C-terminus of the receptor ([13], a kind gift of Dr. Timothy Hla, Cornell University Medical College) using Lipofectamine 2000 (Invitrogen, Carlsbad, CA) according to the manufacturer's instructions. Transfected cells were selected in G418 (0.5 mg/ ml, Life Technologies, Gaithersburg, MD). The IEC-6 cell line was obtained from the American Type Culture Collection (Rockville, MD) at passage 13; passages 16-21 were used in all experiments. IEC-6 cells were maintained in a humidified 37 °C incubator in an atmosphere of 90% air and 10% CO_2. The IEC-6 cell growth medium consisted of Dulbecco's modified Eagle medium supplemented with 5% heat-inactivated FBS, 10 μg/mL insulin, and 50 μg/mL gentamicin.

2.3. Calcium mobilization assays

HTC4 cells stably expressing $S1P_{1-4}$, or transiently expressing either $S1P_5$ or vector were plated in poly-L-lysine coated 96-well microplates (25,000 cells/well) and cultured overnight. The culture medium was replaced with Krebs buffer for 2 - 3 h before assays. The transfected cells were loaded with Fura-2/AM in Krebs buffer containing 0.001% pluronic acid for 30 min, and rinsed with Krebs buffer before measuring Ca^{2+} mobilization. For CHO cells stably expressing P2Y10/Gα16, the cells were plated in 96-well microplates (35,000 cells/well); the next day the cells were loaded with Fura-2/AM in Krebs buffer containing 0.001% pluronic acid for 1 h, and rinsed with Krebs buffer before measuring Ca^{2+} mobilization. The Ca^{2+} responses were measured using a Flex Station II fluorescent plate reader (Molecular Devices, Sunnyvale, CA). The ratio of peak emissions at 510 nm after 2 min of ligand addition was determined for excitation wavelengths of 340 nm/380 nm. All samples were run in triplicate, and assays were performed at least two times for each receptor. The responses were measured and reported in terms of maximal activation (E_{max}) and potency (EC_{50}) ± standard deviation (SD).

2.4. Receptor desensitization assays

HTC4 cells stably expressing $S1P_1$ were cultured overnight, and the next day the medium was replaced with Krebs buffer containing 300 nM compound or vehicle (300 nM charcoal-stripped BSA). After 2 h, cells were loaded with Fura-2/AM in Krebs buffer containing 0.001% pluronic acid for 30 min, and rinsed with Krebs buffer before measuring calcium mobilization.

2.5. Fluorescence confocal microscopy

HEK293 cells stably transfected with $S1P_1$-eGFP were plated on poly-L-lysine coated glass cover slips in 24-well plates (10^5 cells/well) and cultured overnight. The next day, cellular media was replaced with serum-free media for 3 h, and cells were treated with vehicle (100 nM charcoal-stripped BSA) or compounds for 30 min. Cells were either washed in ice cold PBS and fixed for 15 min in 100% methanol at -20°C, or the cells were rinsed twice with serum-free media and incubated for 2 h in serum-free media that contained 15 μg/mL of cycloheximide to prevent new protein synthesis, then fixed in methanol. Microscopy was performed using a Zeiss LSM 5 Pascal laser-scanning confocal microscope.

2.6. Quantitative PCR

The gene-specific primers used are listed in Supplemental Table 1. Total RNA was extracted from IEC-6 cells using TRIzol LS reagent (Invitrogen, Carlsbad, CA). Total RNA was digested by DNase I and used as a template for subsequent cDNA synthesis by random primers using the First Strand Synthesis kit (Invitrogen). The resulting cDNA was used as a template for real-time PCR. Amplification was performed for 40 cycles at 15 s at 95 °C and 60 s at 60 °C using an ABI Model 7300 Real Time PCR machine (Foster City, CA). The data were analyzed by the delta Ct method (http://dorakmt.tripod.com/genetics/realtime.html). The expression level of each S1P or LPA receptor was normalized to β-actin expression.

2.7. ATX assay

The enzyme kinetic mechanisms by which (*R*)-ene and (*S*)-ene inhibited recombinant ATX-mediated hydrolysis of FS-3 were determined by varying the concentration of the substrate (FS-3) in the presence of three concentrations of each inhibitor. The final concentrations of inhibitors used were 0, 0.3, and 1.2 μM for (*R*)-ene, and 0, 0.75, and 3.0 μM for (*S*)-ene. The FS-3 concentrations ranged from 0.3 μM to 20 μM. The buffer used for all assays contained 1 mM $MgCl_2$, 1 mM $CaCl_2$, 3 mM KCl, 140 mM NaCl, 50 mM TRIS, pH 8.0, and 15 μM fatty acid free BSA. All assays were carried out in 96-well, half-area plates (Corning Inc., Corning, NY) at 37°C in a BioTek Synergy-2 plate reader (Winooski, VT) with excitation and emission wavelengths of 485 and 538 nm, respectively. Kinetic data including V_{max} and K_m were determined using KaleidaGraph 4.0 (version 4.03, Synergy Software, Reading, PA) after the plots of initial velocities versus substrate concentration in the absence or presence of inhibitors were fit to the following equation $y = m_1*m_2*x/(1 + m_2*x)$, where $K_m = 1/m_2$; $V_{max} = m_1$. The average K_m for ATX-mediated FS-3 hydrolysis was determined to be 2.7 ± 0.7 μM and was used in the following calculations. The mechanism of inhibition was established by determining K_i and K_i' with the lowest averaged percent residuals for each mechanism derived from curve fitting using the Michaelis-Menten equations for competitive, uncompetitive, mixed-mode, and non-competitive inhibition. A simultaneous non-linear regression was used for each model with WinNonLin® 6.1 (Pharsight, Mountain View, CA). The K_i and K_i' values represent compound affinity for the free enzyme and the enzyme-substrate complex, respectively [14].

For competitive inhibition: $V_o = \frac{V_{max}[S]}{\alpha K_m + [S]}$, where $\alpha = 1 + \frac{[I]}{K_i}$

For non-competitive inhibition (α = α'), therefore: $V_o = \frac{V_{max}[S]}{\alpha(K_m + [S])}$

For uncompetitive inhibition: $V_o = \frac{V_{max}[S]}{K_m + \alpha'[S]}$, where $\alpha' = 1 + \frac{[I]}{K_i'}$

For mixed-mode inhibition: $V_o = \frac{V_{max}[S]}{\alpha K_m + \alpha'[S]}$

2.8. Whole blood lymphocyte counting

The procedures were reviewed and approved by the IACUC of the University of Tennessee Health Science Center. Groups consisting of a minimum of six 10-12 week-old C57BL/6 female mice (Charles River Laboratories) received 1 mg/kg of the test compound dissolved in 5% hydroxypropyl-β-cyclodextrin via intraperitoneal injection. Retroorbital blood was collected before treatment, and for 6 h and 24 h after treatment, in Microvette CD300 K2E vials (Sarstedt). Lymphocyte counts using the EDTA-anticoagulated blood were determined using a Hemavet FS hematological analyzer (Drew Scientific).

2.9. DNA fragmentation ELISA

IEC-6 cells were grown in 48-well culture plates for 24 h, and then cultured in serum-free media overnight. Cells were pretreated with vehicle or compound for 15 min before treatment with camptothecin (20 μM) for 5 h. In some experiments, the cells were incubated overnight with PTX (100 ng/mL) before pretreatment. Apoptosis was determined using a Cell Death Detection ELISA^{PLUS} kit (Roche Diagnostics, Penzberg, Germany) according to the manufacturer's instructions. Protein concentration was measured using the M-Per mammalian protein extraction reagent (Thermo Scientific) followed by the BCA Protein Assay Kit (Pierce Biotechnology).

2.10. Immunoblot analysis

IEC-6 cells were serum starved 24 h before treatment with the test compounds. Some dishes were treated with 100 ng/mL PTX during serum starvation. After the treatment, the cells were washed twice with PBS, lysed in 100 μL of SDS-PAGE sample buffer supplemented with 1% protease inhibitor cocktail and phosphatase inhibitor cocktail (Sigma-Aldrich), and denatured for 10 min at 95°C. An aliquot of 15 μg protein per sample was separated using SDS-PAGE and transferred to PVDF membranes. Membranes were blocked with 5% non-fat milk for 2 h and incubated with the primary antibodies to pERK1/2, ERK1/2, pAKT, AKT (Cell Signaling Technology), and diluted 1:1000 in 5% BSA in 25 mM TRIS (pH 8.0), 137 mM NaCl, 2.7 mM KCl, 0.1% Tween 20 buffer (TBST) overnight at 4°C. The membranes were incubated with the secondary antibody for 2 h at room temperature (anti-rabbit-HRPO, Promega, 1:20,000 in 5% milk-TBST), washed three times with TBST, and visualized by the SuperSignal detection system (Pierce Biotechnology). Band intensities were quantified using NIH ImageJ software.

2.11. Statistical analysis

All experiments were repeated at least three times. Student's t-test and ANOVA was used to determine significant differences ($p < 0.05$) between the data sets. Dose-response curves were fitted using the statistical suite of Kaleidagraph software (Synergy Software).

3. Results

3.1. Pharmacological characterization of FTY720 phosphonates on S1P receptors

Based on ligand-induced [^{35}S]-GTPγS binding assays, FTY720-P is known to activate $S1P_1$, $S1P_3$, $S1P_4$, and $S1P_5$ of the five EDG-family S1P receptors [2,15]. The rat hepatoma cell line HTC4 does not endogenously respond to S1P with Ca^{2+} mobilization [12]. To

assess the activity of the FTY720-phosphonate analogues on the EDG-family S1P receptors, we performed Ca^{2+} mobilization assays using HTC4 cells stably expressing $S1P_{1-4}$ [12]. For the $S1P_5$ receptor subtype, HTC4 cells were transiently transfected with $S1P_5$ and $G\alpha_{qz5}$. Coexpression of the chimeric G protein $G\alpha_{qz5}$ allowed $S1P_5$ to couple to $G\alpha_q$-mediated Ca^{2+} mobilization. HTC4 cells expressing each receptor subtype or vector were treated with increasing concentrations of S1P, FTY720-P, or the phosphonate analogues, and the efficacy (E_{max}) and potency (EC_{50}) of the Ca^{2+} responses were measured (Fig. 2, A-F). Vector-transfected cells were unresponsive to S1P, FTY720-P, or analogues in this assay (Fig. 2A). S1P activated Ca^{2+} transients in HTC4 cells expressing each individual $S1P_{1-5}$ receptor and was a full agonist. $S1P_1$-transfected cells were the most responsive to FTY720-P; the $S1P_1$ transfectants were activated by FTY720-P to 85% of the maximal S1P-induced activation and displayed a similar potency as for S1P (4 ± 1 nM for S1P *vs* 5 ± 1 nM for FTY720-P; for EC_{50} and E_{max} values; see Table I). (*R*)-FTY720-phosphonate and (*R*)-ene were full agonists, whereas (*S*)-FTY720-phosphonate was a partial agonist of $S1P_1$ (Fig. 2B). (S)-ene did not activate $S1P_1$ at concentrations up to 10 μM. Cells transfected with either $S1P_3$ or $S1P_4$ showed smaller Ca^{2+} responses to FTY720-P relative to S1P. In the case of $S1P_3$, the efficacy of FTY720-P was only 23% and the EC_{50} value was increased more than ten-fold relative to S1P (Fig. 2D). For $S1P_4$, the EC_{50} value of FTY720-P was increased to > 500 nM *vs* 6 ± 2 nM for S1P. All four chiral phosphonate and vinylphosphonate analogues failed to activate $S1P_2$, $S1P_4$, and $S1P_5$ (Fig. 2, C, E and F). (*S*)-FTY720-phosphonate and (*S*)-ene were inactive against $S1P_3$ at concentrations up to 10 μM, whereas *(R)*-FTY720-phosphonate and (*R*)-ene were low efficacy agonists (E_{max} < 20% of S1P), eliciting responses only at concentrations above 300 nM (Fig. 2D). $S1P_2$-transfected cells only responded to micromolar concentrations of FTY720-P (Fig. 2C), as expected from previous data showing that FTY720-P does not activate $S1P_2$ [2] The $S1P_5$-transfected cells were not responsive to FTY720-P in our assays (Fig. 2F). (S)-ene failed to activate any of the five S1P receptors when applied at concentrations up to 10 μM, even though the same receptors responded to nanomolar concentrations of S1P.

Recently, the P2Y10 receptor was found to be a GPCR with dual specificity for LPA and S1P [16]. We measured the Ca^{2+} responses to LPA, S1P, FTY720-P and analogues in CHO cells stably transfected with $G\alpha_{16}$ plasmid alone or with a P2Y10 receptor fused to the $G\alpha_{16}$ protein (Fig. 2, G and F). CHO cells transfected with $G\alpha_{16}$ alone showed a response to LPA at concentrations of 300 nM and above, indicating the presence of an endogenous LPA receptor. However, there was no response to S1P, FTY720-P, or any of the analogues we tested (Fig. 2G). LPA was a full agonist of P2Y10, with an EC_{50} of 51 ± 14 nM. S1P was a weaker agonist in our Ca^{2+} mobilization assays than LPA, with an EC_{50} > 500 nM, and the maximal response at 10 μM S1P was only 60% of the maximal LPA-induced response. The CHO cells stably transfected with the P2Y10/$G\alpha_{16}$ fusion protein did not mobilize calcium in response to FTY720-P or any of the phosphonate or vinylphosphonate analogues (Fig. 2H).

3.2. (S)-ene is a pan antagonist of the EDG family S1P receptors

Because (*S*)-ene uniquely failed to activate any of five EDG-family S1P receptors or P2Y10, we examined whether it may function as an antagonist. We tested it for antagonism at $S1P_{1-5}$ and P2Y10 receptors. In these experiments, increasing concentrations of (*S*)-ene were added together with a concentration of S1P near the EC_{70} for each receptor subtype, and Ca^{2+} transients were monitored. (*S*)-ene inhibited the S1P-induced Ca^{2+} response in $S1P_1$, $S1P_2$, $S1P_3$, $S1P_4$, and $S1P_5$-expressing HTC4 cells in a dose-dependent manner, although with different potency and efficacy (Fig. 3 A-C, and Table 2). (S)-ene was a full antagonist of $S1P_1$, $S1P_3$, and $S1P_4$ with K_i values of 384 nM, 39 nM, and 1190 nM, respectively, and was a partial antagonist of $S1P_2$ and $S1P_5$. At concentrations up to 30 μM,

(S)-ene had no inhibitory effect on P2Y10 when co-applied with S1P. The mechanism of antagonism of (*S*)-ene against $S1P_1$ and $S1P_3$ appears consistent with competitive inhibition, as it dose dependently shifted the S1P dose response curve to the right without affecting E_{max} (Fig. 4A). Schild analysis [17] yielded a pKb of 7.10 M (average residual error 1.09) for $S1P_1$ and a pKb of 7.61 M (average residual error 0.62) for $S1P_3$.

Although an agonist of the $S1P_1$ receptor, FTY720-P acts as a functional antagonist of $S1P_1$ by causing internalization of the receptor from the cell surface, followed by intracellular sequestration and degradation of the receptor leading to long-lasting desensitization of the $S1P_1$ response. To further characterize the biological effects of (*R*)- and (S)-FTY720-vinylphosphonates, we tested whether preincubation of $S1P_1$-expressing HTC4 cells with these ligands causes desensitization of the $S1P_1$ response. To examine the effect of pretreatment on the dose-response relationship to the natural ligand, we treated $S1P_1$-expressing HTC4 cells with 300 nM S1P, FTY720-P, (*S*)-ene, (*R*)-ene, or vehicle for 2 h, and then replaced the medium and measured the response to increasing concentrations of S1P (Fig. 4B). Preincubation of the cells with vehicle did not affect the dose-response properties of $S1P_1$. Pretreatment of the cells with S1P or FTY720-P completely desensitized the S1P response. Similarly, (*R*)-ene preincubation caused desensitization of the $S1P_1$ receptor, which is consistent with its agonist properties at the $S1P_1$ receptor. In contrast, (*S*)-ene preincubation had almost no effect on the S1P dose-response curve, which is consistent with the mode of action of an antagonist.

$S1P_1$ is rapidly internalized following receptor activation. To directly determine the effects of the (*R*)- and (*S*)-ene compounds on $S1P_1$ receptor internalization, we applied these compounds as well as FTY720-P or S1P to HEK293 cells stably transfected with a chimeric $S1P_1$ receptor C-terminally fused to eGFP, and then examined the effect of these ligands on receptor localization by confocal microscopy. Incubation of cells with 100 nM S1P or 10 nM FTY720-P for 30 min caused internalization of the receptor, resulting in a punctuate localization away from the plasma membrane (Fig. 5). Consistent with its agonist mode of action, (*R*)-ene (100 nM) caused a similar internalization of the $S1P_1$-eGFP receptor. However, treatment with 100 nM (*S*)-ene failed to cause redistribution of $S1P_1$-eGFP from the plasma membrane, consistent with its antagonist action at $S1P_1$.

FTY720-P causes a more prolonged downregulation of surface expression of $S1P_1$ than S1P, favoring intracellular sequestration followed by polyubiquitination and proteasomal degradation of the receptor, rather than recycling of the receptor back to the plasma membrane [3]. After a 30-min exposure, we washed out the test compounds and incubated the cells at 37°C for 2 h to examine recycling of the $S1P_1$ receptor to the plasma membrane; cycloheximide was included in the incubations to prevent new protein synthesis. In agreement with previously reported studies [3], cells treated with FTY720-P retained a punctuate intracellular FTY720-P localization after 2 h, whereas in cells treated with S1P the $S1P_1$ receptor had recycled back to the plasma membrane. Similarly to the S1P-treated cells, the $S1P_1$ receptor recycled back to the plasma membrane after 2 h in cells treated with (*R*)-ene, indicating that this compound more closely resembles S1P than FTY720-P in its agonist effect on receptor downregulation.

We hypothesized that *(S)*-ene, as an $S1P_1$ antagonist, should disrupt the egress of lymphocytes from the secondary lymphoid organs and lead to peripheral lymphopenia. Thus *(R)*-ene, as a result of its desensitizing action, should mimic the effects of S1P and FTY720-P on peripheral blood lymphocyte counts. To test this, we injected C57BL/6 mice with 1 mg/kg of FTY720-P, *(S)*-ene, *(R)*-ene, or vehicle and determined the peripheral lymphocyte counts 6 h later. FTY720-P and *(R)*-ene caused an approximately 90% decrease in circulating lymphocytes, whereas *(S)*-ene only caused a decrease of approximately 20%

(Fig. 6). By 24 h, circulating lymphocyte counts had been restored to pretreatment levels in mice injected with *(S)*-ene or *(R)*-ene, whereas mice injected with FTY720-P continued to be deficient in circulating lymphocytes. For all of the treatment groups, neutrophil, platelet, and red blood cell counts were not significantly changed compared to their pre-treatment values (data not shown).

S1P may act as a survival for many cell types [18,19]. Both S1P and FTY720-P have been shown to protect oligodendrocyte progenitor cells from apoptotic cell death in response to growth factor withdrawal, and FTY720-P was also shown to be cytoprotective in response to pro-apoptotic cytokines and microglial activation [20,21]. We assessed the ability of pretreatment with the FTY720-P analogues to protect rat epithelial IEC-6 cells from apoptotic cell death in response to camptothecin-induced DNA fragmentation. Pretreatment with the (*R*)- or (*S*)-ene analogues showed a significant and dose-dependent reduction in DNA fragmentation elicited by 20 μM camptothecin (Fig. 7A). The dose-response relationship of the antiapoptotic effect showed an inverse bell-shape curve with maximal protection for both compounds at 300 nM. We performed quantitative real-time PCR to determine the receptor mRNA profile of S1P and LPA receptors in this cell type. We found that IEC-6 cells express appreciable levels of several LPA receptors, with P2Y5 and LPA_1 being the predominant subtypes expressed, followed in rank order by lower levels of LPA_4, LPA_3, GPR87, and LPA_2. Among the S1P receptors, IEC-6 cells express high levels of $S1P_2$ mRNA and a much lower level of $S1P_5$ transcripts (Fig. 7B). Neither of these S1P receptors present in IEC-6 cells are activated by the (*R*)-ene or (*S*)-ene analogues of FTY720-P (Fig. 2), suggesting the cytoprotective effect of these compounds is mediated by another (yet unidentified) molecular target present in this cell line. To examine if this target is sensitive to PTX treatment, IEC-6 cells were pretreated with 100 ng/mL PTX overnight prior to induction of apoptosis with 20 μM camptothecin and cotreatment with 300 nM (*R*)- or (*S*)-ene. PTX treatment partially inhibited the antiapoptotic action of both compounds (Fig. 7C) but also augmented apoptosis in the controls preventing a clear interpretation of the effect.

Inhibition of apoptosis by (*R*)-ene or (*S*)-ene, the former of which is agonist, the latter antagonist of S1P receptors is difficult to reconcile if one only considers these S1P receptors as the singular targets of the two compounds. One way to establish the engagement of additional target(s) of the vinyl phosphonate analogs was to examine whether it activated prosurvival kinase pathways involved in IEC-6 cell apoptosis. Both enantiomers elicited ERK1/2 and AKT phosphorylation within minutes of application that was significant as early as 2.5 min and peaked between 5-15 minutes (Fig. 8A & B). PTX treatment overnight partially inhibited ERK1/2 activation in response to S1P, but had no significant effect on ERK1/2 activation in response to (*R*)-ene or (*S*)-ene (Fig. 8C).

Because neither of the S1P receptors present in IEC-6 cells was activated by the (*R*)-ene or (*S*)-ene and there is high structural similarity between S1P and LPA, we examined the possibility that LPA receptors may function as cellular targets of (*R*)-ene or (*S*)-ene. We tested the effects of (*R*)- and (*S*)-ene on Ca^{2+} mobilization in cells transfected with $LPA_{1,2,3,4,5}$ and the putative LPA receptor GPR87. We were unable to detect (*R*)- or (*S*)-ene dependent Ca^{2+} mobilization responses in cells transfected with any of the LPA receptors, although LPA could elicit Ca^{2+} transients from each of these receptors (data not shown).

ATX, an enzyme with lysophospholipase D activity that cleaves the choline group from lysophosphatidylcholine and sphingophosphorylcholine, is a target of FTY720-P [8]. Since (*R*)- and (*S*)-FTY720-vinylphosphonates are similar in structure to FTY720-P, we evaluated these analogues for inhibition of ATX using FS-3 as a model enzyme substrate. (*R*)-ene inhibited ATX by an uncompetitive mechanism ($K_i = K_{i'} = 0.92$ μM) whereas (*S*)-ene showed a competitive mechanism of enzyme inhibition with $K_i = 1.0$ μM.

3. DISCUSSION

FTY720-P has generated a great deal of interest as an immunosuppressive agent. FTY720-P desensitizes the $S1P_1$ receptor, which is expressed on lymphocytes and is essential for lymphocyte egress from secondary lymphoid organs. Many pharmaceutical and academic laboratories have searched for agents similar to FTY720-P. The first exploration of chiral analogues of FTY720 was reported by Kiuchi et al [22] noting that the *R* enantiomer of 2-amino-4-(4-heptoxyphenyl)-2-methylbutanol (AAL) was highly effective in decreasing T-cell activity whereas its *S* enantiomer was inactive up to 1 mg/kg. Brinkmann and colleagues [15] showed that the lack of in vivo activity of *(S)*-AAL-phosphate was due to its approximately 100-fold weaker agonist action at select S1P receptors. These authors also showed that *(S)*-AAL was not phosphorylated by sphingosine kinase 1, a finding that was extended by Don et al. to sphingosine kinase 2 [23].

There is substantial current interest in developing FTY720 mimics. We recently reported the chiral syntheses of four chiral phosphonate analogues of FTY720-P [11], together with a preliminary characterization of the unexpected stereoselective properties of (*R*)- and (*S*)-FTY720-vinylphosphonates [24]. Therefore, we have now carried out a comprehensive pharmacological characterization of these compounds at previously established targets of FTY720. Our studies using heterologously expressed individual S1P receptor-mediated Ca^{2+} mobilization assays in HTC4 cells show that the chiral FTY720 phosphonates elicited enantioselective activation patterns. Whereas FTY720-P activates Ca^{2+} responses through $S1P_1$, $S1P_3$, and $S1P_4$, its phosphonate analogues became selective for $S1P_1$ (Table I). Furthermore, neither FTY720-P nor the analogues we studied here activated the putative dual-specificity LPA/S1P receptor P2Y10 (Fig. 2H). Of note is that G16α vector-transfected CHO cells did not show any Ca^{2+} response to S1P, although they did show a modest response to LPA (Fig. 2G). These observations are consistent with the hypothesis that P2Y10 is activated by S1P. Because the Gα16 vector cells were also responsive to LPA, the issue of LPA responsiveness of this receptor will require additional study. However, the decreased EC_{50} and higher E_{max} values clearly support the hypothesis that P2Y10 is also responsive to submicromolar concentrations of LPA. Our study was not designed to resolve these issues; nevertheless, the data obtained with these ligands from P2Y10-expressing CHO cells deserves mention, especially because FTY720-P does not activate this receptor.

Of the two vinylphosphonate analogues, *(S)*-ene failed to activate any of the EDG-family S1P receptors whereas *(R)*-ene was a selective partial agonist of $S1P_1$. Further characterization of *(S)*-ene revealed that it inhibited the five S1P receptors and was a full antagonist at three of the five S1P receptors. Based on its 39 nM K_i value at the $S1P_3$ receptor, *(S)*-ene is the most potent inhibitor of this receptor subtype reported to date, exceeding the inhibitory potencies of other synthetic analogues. For example, a K_i value of 110 nM of TY-52156 was reported very recently [25], and an earlier study reported a K_i value of 1.04 μM for VPC23019 [26], although the latter compound also activated $S1P_4$ and $S1P_5$. Furthermore, *(S)*-ene was found to be a reasonably potent inhibitor of $S1P_1$ (K_i = 384 nM) and $S1P_4$ (K_i = 1190 nM) in our cellular assays. Further characterization of *(S)*-ene at $S1P_1$ showed an inhibition mechanism that was competitive (Fig. 4A). Consistent with its antagonist properties, *(S)-ene* did not induce $S1P_1$ receptor desensitization or internalization of a $S1P_1$-eGFP chimeric protein.

FTY720-P and S1P both cause peripheral blood lymphopenia by sequestering lymphocytes in the secondary lymphoid organs [2]. One hypothesis for this effect is based on the S1P gradient between lymph and blood sensed by $S1P_1$ receptors expressed on lymphocytes as a chemoattractant gradient [27,28]. Based on this model, inhibition of $S1P_1$ function either by competitive inhibition via *(S)*-ene or by receptor downregulation via *(R)*-ene should mimic

the actions of FTY720-P. We tested this hypothesis and found that both *(R)*- and *(S)*-ene significantly decreased peripheral blood lymphocyte counts. However, *(S)*-ene was much less effective than *(R)*-ene, which is consistent with the several hundred nanomolar concentration of S1P in plasma [27] that competes against *(S)*-ene. Pharmacokinetic profiling of these compounds will be necessary to ascertain the validity of these two hypotheses. Tonelli and colleagues' in an accompanying paper [29] have shown that *(S)*-ene is an inhibitor of sphingosine kinase 1, and at high micromolar concentrations it induces proteasomal degradation of sphingosine kinase 1, in turn leading to apoptosis after 24-h drug treatment. Thus, a potential inhibition of S1P production could also contribute to the lymphopenic effect of *(S)*-ene but not *(R)*-ene; this should be tested in future experiments.

In the non-transformed rat intestinal crypt-like cell line IEC-6, both enantiomers of FTY720-vinylphosphonates inhibited camptothecin-induced apoptosis and activated the prosurvival kinases ERK1/2 and AKT (Figs. 7 & 8). The attenuation of DNA fragmentation showed a bell-shaped dose-response curve, with maximal efficacy in the submicromolar range. This may seem to be contrary to the proapoptotic effect of *(S)*-ene in human pulmonary artery smooth muscle cells and androgen-independent LNCaP-AI prostate cancer cells described in the accompanying paper by Tonelli et al. . However, these findings are not mutually exclusive but rather point to the complexity of the molecular signaling targets of the FTY720 family of compounds. At concentrations above 1 μM, *(S)*-ene no longer showed an attenuation of DNA fragmentation, which would be consistent with the increasing inhibition of sphingosine kinase 1 leading to increased apoptosis. Furthermore, the duration of the apoptosis protection assay is only 5 h, and the downregulation of sphingosine kinase 1 was manifested much later (at 24 h). Another crucial difference between our observations and those of Tonelli and colleagues is that whereas in IEC-6 cells we see a time- and dose-dependent activation of ERK1/2 and AKT there was no ERK1/2 activation detected in human pulmonary artery smooth muscle cells. In IEC-6 cells, we did not find PTX-sensitivity in ERK1/2 activation, although the inhibition of camptothecin-induced DNA fragmentation was attenuated by PTX. However, PTX alone had a similar effect in camptothecin-treated cells, which precludes the interpretation of a PTX-sensitive target for the two FTY720-vinylphosphonates. In this context, one must recognize that many targets of FTY720, and potentially those of FTY720-P, are involved in both pro- and anti-apoptotic signaling, including sphingosine 1-phosphate lyase [30], sphingosine kinase 1 [4], phospholipase A_2 [5], ceramide synthase [6,7,9,10], as well as lysophospholipase D/ autotaxin (ATX) [8]. Thus, at the present time the cell-type specific targets mediating ERK1/2 and AKT activation remain unknown and will be subject of further studies.

Autotaxin is a plasma lysophospholipase D that generates LPA from LPC in blood [31,32]. ATX also cleaves sphingosylphosphorylcholine *in vitro* and generates S1P [33]. ATX shows product feedback inhibition, and S1P and LPA both inhibit its activity [34]. As FTY720-P has been shown to inhibit ATX [8], we tested whether *(R)*- and/or *(S)*-ene are also inhibitors. We found that both FTY720-vinylphosphonates were potent inhibitors of recombinant ATX with IC_{50} values in the micromolar-submicromolar range. Interestingly, the mechanism of inhibition showed enantiomer-specific differences; *(S)*-ene was a competitive mode inhibitor (Ki = 1 μM) whereas *(R)*-ene acted by a non-competitive mechanism on ATX activity (Ki= 0.92 μM). Thus, *(S)*-ene is a novel compound: it inhibits ATX and sphingosine kinase 1 without stimulating any of the S1P or LPA receptors. These combined properties of *(S)*-ene make it potentially applicable for the inhibition of ATX generated by highly aggressive metastatic tumors [35]. It may also block tumor angiogenesis mediated by sphingosine kinase 1 and $S1P_1$ [36].

4. CONCLUSIONS

The present findings indicate that (*S*)-FTY720 vinylphosphonate is a pan antagonist of the EDG-family S1P receptors, whereas, (*R*)-FTY720 vinylphosphonate is an agonist of the $S1P_1$ receptor. (*R*)-FTY720 vinylphosphonate inhibited ATX by a non-competitive mechanism whereas (*S*)-FTY720 vinylphosphonate showed a competitive type enzyme inhibition in the low micromolar range. Both compounds activated ERK1/2 and AKT in IEC-6 nontransformed rat gut epithelial cells and attenuated camptothecin-induced DNA fragmentation in the submicromolar range but were ineffective at higher concentrations. These compounds offer potential utility on dissecting the mechanism of action and multiple targets of FTY270.

Supplementary Material

Refer to Web version on PubMed Central for supplementary material.

Acknowledgments

This work was supported by NIH Grants AI80405 (to GT), CA921160 (to GT) and HL083187 (to RB), and CRUK 23158/A7536 (to NJP). The authors thank Dr. Betsey Tolley for her help with the statistical analysis and Danny Morse for his assistance with the illustrations.

Abbreviations

FTY720-P	(*S*)-FTY720-phosphate
(*S*)-ene	(*S*)-FTY720-vinylphosphonate
(*R*)-ene	(*R*)-FTY720-vinylphosphonate
S1P	sphingosnie 1-phophate
LPA	lysophosphatidic acid
ATX	autotaxin

References

1. Brinkmann V. Br J Pharmacol. 2009; 158(5):1173–1182. [PubMed: 19814729]
2. Mandala S, Hajdu R, Bergstrom J, Quackenbush E, Xie J, Milligan J, Thornton R, Shei GJ, Card D, Keohane C, Rosenbach M, Hale J, Lynch CL, Rupprecht K, Parsons W, Rosen H. Science. 2002; 296(5566):346–349. [PubMed: 11923495]
3. Oo ML, Thangada S, Wu MT, Liu CH, Macdonald TL, Lynch KR, Lin CY, Hla T. J Biol Chem. 2007; 282(12):9082–9089. [PubMed: 17237497]
4. Vessey DA, Kelley M, Zhang J, Li L, Tao R, Karliner JS. Journal of Biochemical and Molecular Toxicology. 2007; 21(5):273–279. [PubMed: 17912702]
5. Payne SG, Oskeritzian CA, Griffiths R, Subramanian P, Barbour S, Chalfant CE, Milstein S, Spiegel S. Blood. 2007; 109:1077–1085. [PubMed: 17008548]
6. Berdyshev EV, Gorshkova I, Skobeleva A, Bittman R, Lu X, Dudek SM, Mirzapoiazova T, Garcia JG, Natarajan V. J Biol Chem. 2009; 284:5467–5477. [PubMed: 19119142]
7. Lahiri S, Park H, Laviad EL, Bittman R, Futerman AH. J Biol Chem. 2009; 284:16090–16098. [PubMed: 19357080]
8. van Meeteren LA, Brinkmann V, Saulnier-Blache JS, Lynch KR, Moolenaar WH. Cancer Lett. 2008; 266(2):203–208. [PubMed: 18378389]
9. Matsuoka Y, Nagahara Y, Ikekita M, Shimnomiya T. Br J Pharmacol. 2003; 138:1303–1312. [PubMed: 12711631]

10. Neviani P, Shantanam R, Oaks JJ, Eiring AM, Notari M, Blaser BW, Liu S, Trotta R, Muthusamy N, Gambacorti-Passerini C, Druker BJ, Cortes J, Marcucci G, Chen CS, Verrils NM, Roy DC, Caliguri MA, Bloomfield CD, Byrd JC, Perotti D. J Clin Invest. 2007; 117:2408–2421. [PubMed: 17717597]
11. Lu X, Sun C, Valentine WJ, Shuyu E, Liu J, Tigyi G, Bittman R. J Org Chem. 2009; 74(8):3192–3195. [PubMed: 19296586]
12. An S, Bleu T, Zheng Y. Mol Pharmacol. 1999; 55(5):787–794. [PubMed: 10220556]
13. Liu CH, Thangada S, Lee MJ, Van Brocklyn JR, Spiegel S, Hla T. Mol Biol Cell. 1999; 10(4):1179–1190. [PubMed: 10198065]
14. Hoeglund AB, Howard AL, Wanjala IW, Pham TC, Parrill AL, Baker DL. Bioorg Med Chem. 2010; 18(2):769–776. [PubMed: 20005724]
15. Brinkmann V, Davis MD, Heise CE, Albert R, Cottens S, Hof R, Bruns C, Prieschl E, Baumruker T, Hiestand P, Foster CA, Zollinger M, Lynch KR. J Biol Chem. 2002; 277(24):21453–21457. [PubMed: 11967257]
16. Murakami M, Shiraishi A, Tabata K, Fujita N. Biochem Biophys Res Commun. 2008; 371(4):707–712. [PubMed: 18466763]
17. Lew MJ, Angus JA. Trends Pharmacol Sci. 1995; 16(10):328–337. [PubMed: 7491710]
18. Cuvillier O, Pirianov G, Kleuser B, Vanek PG, Coso OA, Gutkind S, Spiegel S. Nature. 1996; 381(6585):800–803. [PubMed: 8657285]
19. Radeff-Huang J, Seasholtz TM, Matteo RG, Brown JH. J Cell Biochem. 2004; 92(5):949–966. [PubMed: 15258918]
20. Saini HS, Coelho RP, Goparaju SK, Jolly PS, Maceyka M, Spiegel S, Sato-Bigbee C. J Neurochem. 2005; 95(5):1298–1310. [PubMed: 16313513]
21. Coelho RP, Payne SG, Bittman R, Spiegel S, Sato-Bigbee C. J Pharmacol Exp Ther. 2007; 323(2):626–635. [PubMed: 17726159]
22. Kiuchi M, Adachi K, Kohara T, Minoguchi M, Hanano T, Aoki Y, Mishina T, Arita M, Nakao N, Ohtsuki M, Hoshino Y, Teshima K, Chiba K, Sasaki S, Fujita T. J Med Chem. 2000; 43(15):2946–2961. [PubMed: 10956203]
23. Don AS, Martinez-Lamenca C, Webb WR, Proia RL, Roberts E, Rosen H. J Biol Chem. 2007; 282(21):15833–15842. [PubMed: 17400555]
24. Camp SM, Bittman R, Chiang ET, Moreno-Vinasco L, Mirzapoiazova T, Sammani S, Lu X, Sun C, Harbeck M, Roe M, Natarajan V, Garcia JG, Dudek SM. J Pharmacol Exp Ther. 2009; 331(1):54–64. [PubMed: 19592667]
25. Murakami A, Takasugi H, Ohnuma S, Koide Y, Sakurai A, Takeda S, Hasegawa T, Sasamori J, Konno T, Hayashi K, Watanabe Y, Mori K, Sato Y, Takahashi A, Mochizuki N, Takakura N. Mol Pharmacol. 2010; 77(4):704–713. [PubMed: 20097776]
26. Davis MD, Clemens JJ, Macdonald TL, Lynch KR. J Biol Chem. 2005; 280(11):9833–9841. [PubMed: 15590668]
27. Pappu R, Schwab SR, Cornelissen I, Pereira JP, Regard JB, Xu Y, Camerer E, Zheng YW, Huang Y, Cyster JG, Coughlin SR. Science. 2007; 316(5822):295–298. [PubMed: 17363629]
28. Schwab SR, Pereira JP, Matloubian M, Xu Y, Huang Y, Cyster JG. Science. 2005; 309(5741):1735–1739. [PubMed: 16151014]
29. Tonelli F, Lim KG, Loveridge C, Long J, Pitson SM, Tigyi G, Bittman R, Pyne S, Pyne NJ. Cell Signal. 2010 submitted.
30. Bandhuvula P, Tam YY, Oskouian B, Saba JD. J Biol Chem. 2005; 280(40):33697–33700. [PubMed: 16118221]
31. Tokumura A, Majima E, Kariya Y, Tominaga K, Kogure K, Yasuda K, Fukuzawa K. J Biol Chem. 2002; 277(42):39436–39442. [PubMed: 12176993]
32. Umezu-Goto M, Kishi Y, Taira A, Hama K, Dohmae N, Takio K, Yamori T, Mills GB, Inoue K, Aoki J, Arai H. J Cell Biol. 2002; 158(2):227–233. [PubMed: 12119361]
33. Clair T, Aoki J, Koh E, Bandle RW, Nam SW, Ptaszynska MM, Mills GB, Schiffmann E, Liotta LA, Stracke ML. Cancer Res. 2003; 63(17):5446–5453. [PubMed: 14500380]

34. van Meeteren LA, Ruurs P, Christodoulou E, Goding JW, Takakusa H, Kikuchi K, Perrakis A, Nagano T, Moolenaar WH. J Biol Chem. 2005; 280(22):21155–21161. [PubMed: 15769751]

35. Vidot S, Witham J, Agarwal R, Greenhough S, Bamrah HS, Tigyi GJ, Kaye SB, Richardson A. Cell Signal. 2010; 22(6):926–935. [PubMed: 20100569]

36. LaMontagne K, Littlewood-Evans A, Schnell C, O'Reilly T, Wyder L, Sanchez T, Probst B, Butler J, Wood A, Liau G, Billy E, Theuer A, Hla T, Wood J. Cancer Res. 2006; 66(1):221–231. [PubMed: 16397235]

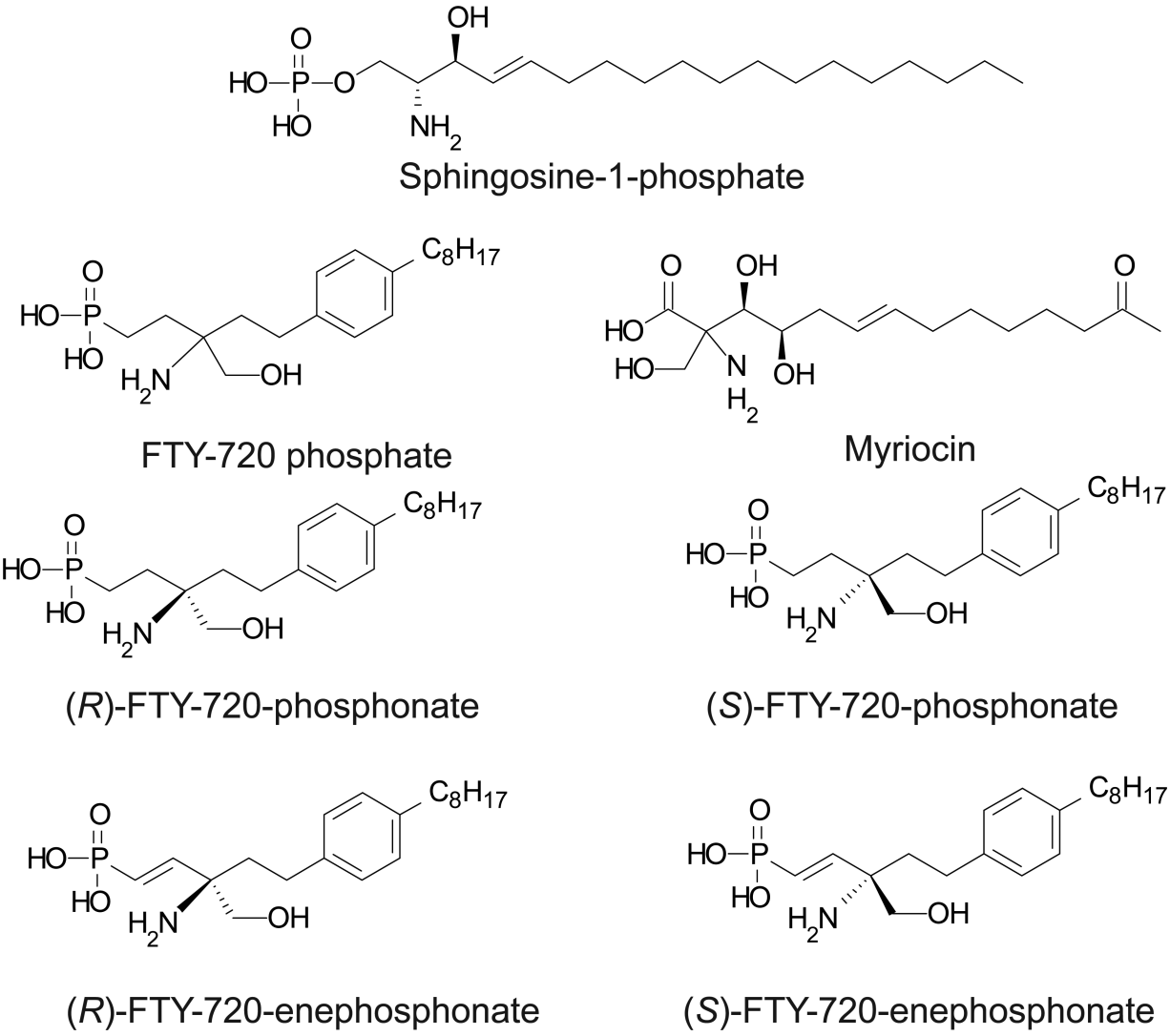

Fig. 1.
Structures of *(S)*-FTY720-P, *(S)*-FTY720-phosphonate, *(R)*-FTY720-phosphonate, *(R)*-FTY720-vinylphosphonate, and *(S)*-FTY720-vinylphosphonate.

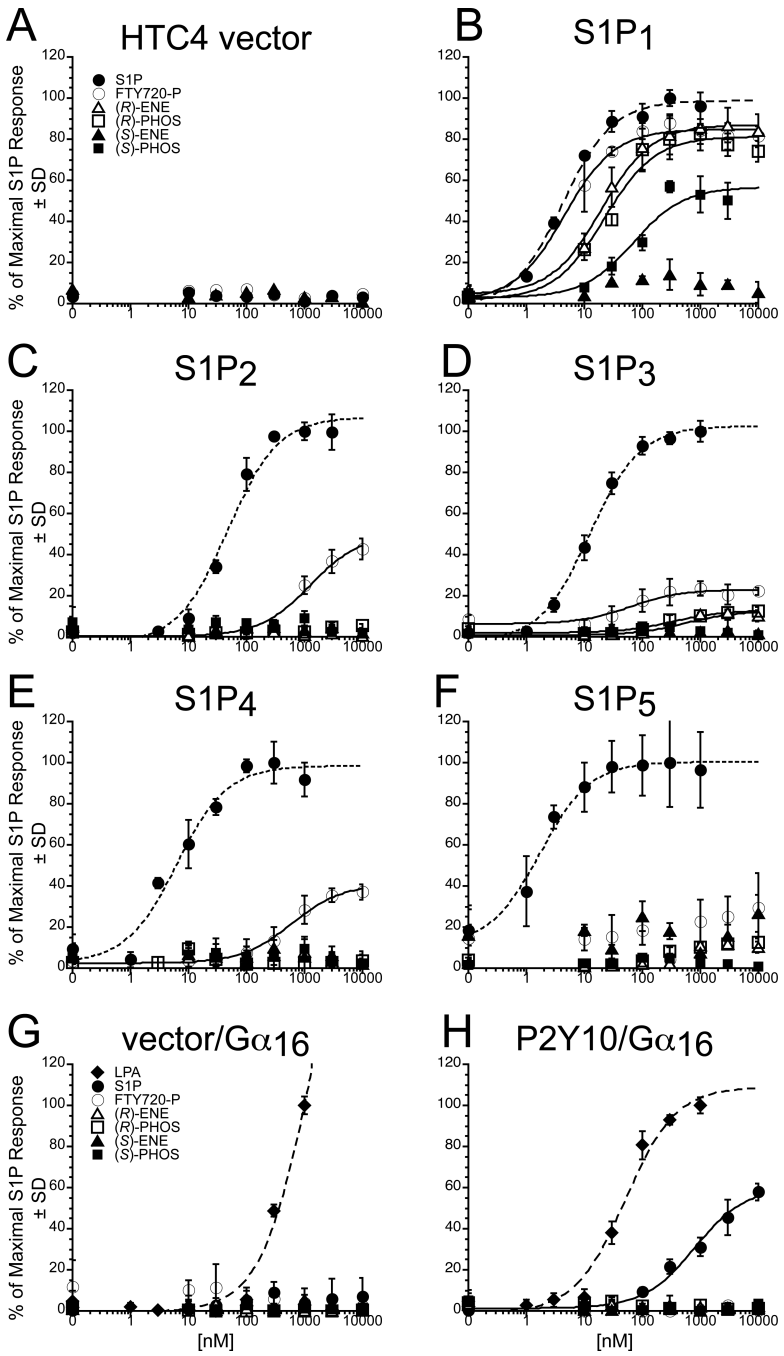

Fig. 2.

Receptor activation of $S1P_{1\text{-}5}$ and P2Y10 in response to S1P, (*S*)-FTY720-P, or analogues (see also Table I). Intracellular Ca^{2+} transients were measured in HTC4 cells transfected with vector (A), $S1P_1$ (B), $S1P_2$ (C), $S1P_3$ (D), $S1P_4$ (E), or $S1P_5$ (F), and in CHO cells stably expressing Gα16 alone (G) or P2Y10/Gα16 (H). In the HTC4 S1P receptor transfectants, 100% represents the maximal Ca^{2+} response to S1P. For the HTC4 vector-transfected cells, that value is normalized to cells stably transfected with $S1P_1$. For CHO cells expressing P2Y10 fused to Gα16 or else Gα16 alone, 100% represents the maximal P2Y10/Gα16 response to LPA. Samples were run in triplicate, and the mean ± SD was plotted.

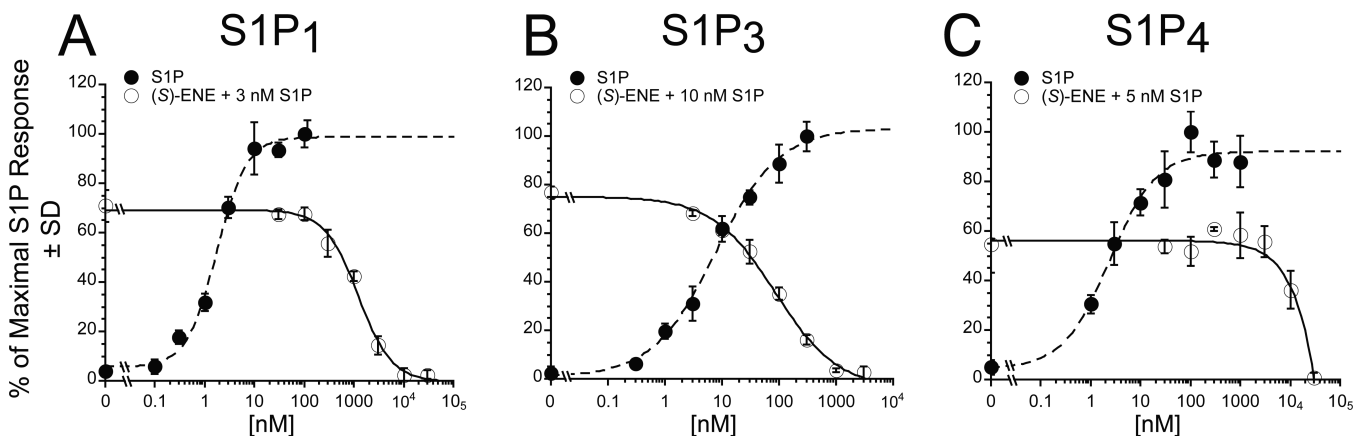

Fig. 3.

(S)-ene dose-dependent inhibition of $S1P_{1,3,and\ 4}$ receptor activation by S1P. Intracellular Ca^{2+} transients were measured in HTC4 cells transfected with $S1P_1$ (A), $S1P_3$ (B), or $S1P_4$ (C). 100% represents the maximal Ca^{2+} response to S1P in the transfected cell line. Samples were run in triplicate, and the mean ± SD was plotted.

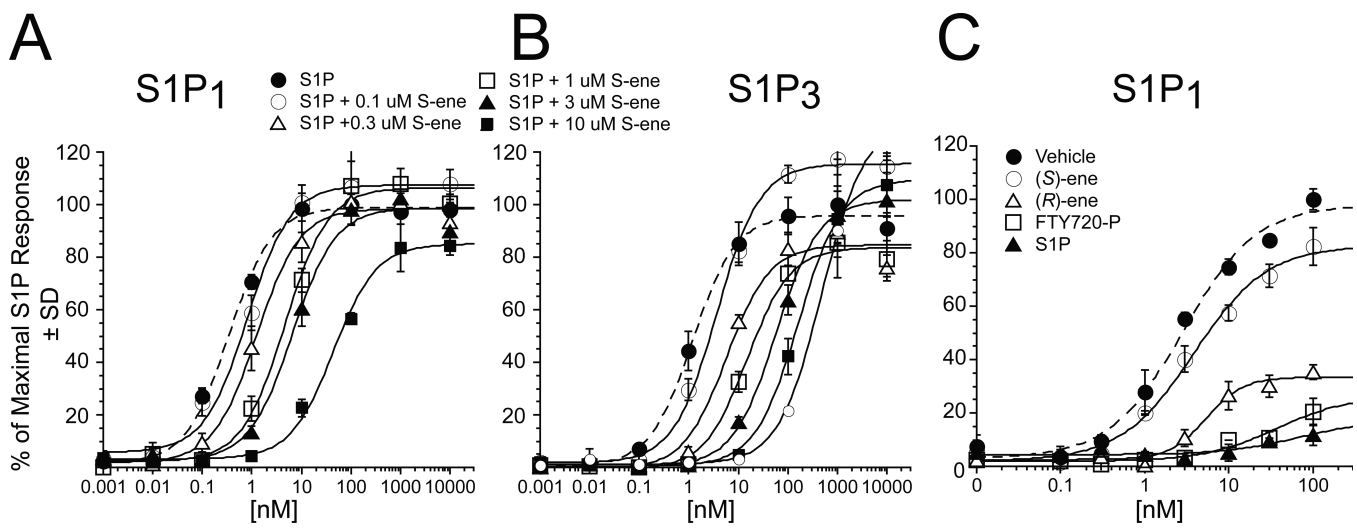

Fig. 4.

Effect of (S)-ene on S1P receptor activation. Competitive inhibition of $S1P_1$ by (S)-ene(Panel A). HTC4 cells expressing the S1P receptor subtypes were exposed to increasing concentrations of S1P in the presence or absence of different concentrations of (*S*)-ene. Data points are the means for triplicate determinations ± SD. Effect of S1P, FTY720-P, (*S*)-ene, or (*R*)-ene preincubation on $S1P_1$ activation (Panel B). Dose response curves were recorded to S1P from $S1P_1$-expressing HTC4 cells preincubated with 300 nM vehicle (BSA), 300 nM each of S1P, FTY720-P, *(R)*-ene, or *(S)*-ene for 2 h. Samples were run in triplicate, and the mean ± SD was plotted.

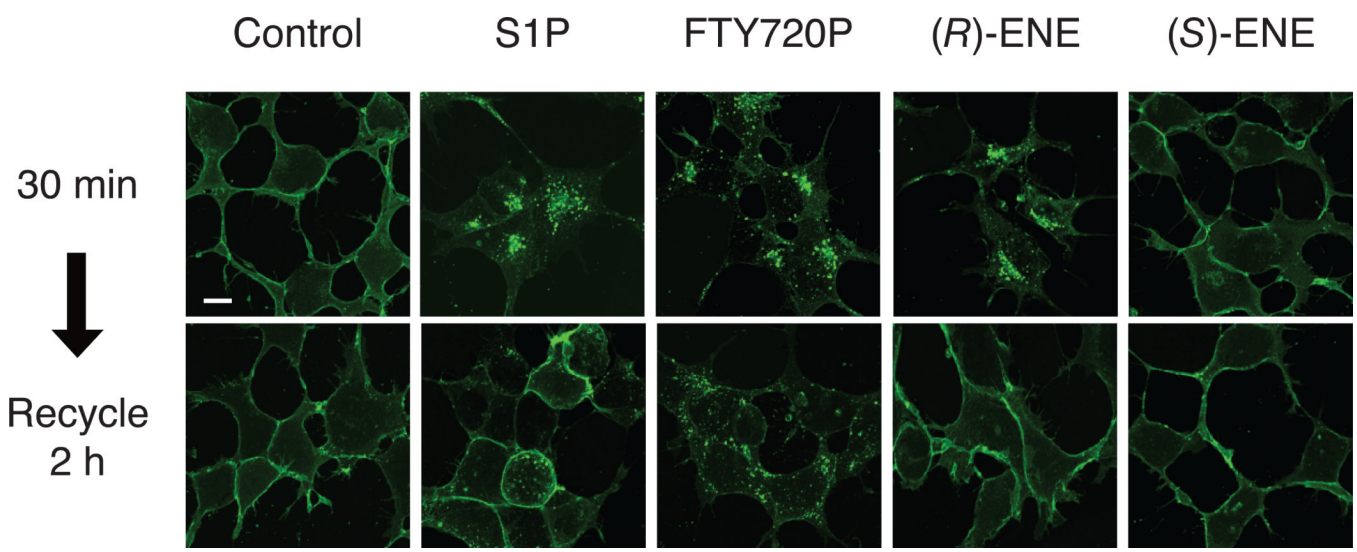

Fig. 5.

Receptor internalization of $S1P_1$-eGFP-transfected HEK293T cells exposed to vehicle control (100 nM BSA), 10 nM FTY720-P, 100 nM S1P, 100 nM *(R)*-ene, or 100 nM *(S)*-ene for 30 min or 2 h. The cells were fixed and viewed using laser-scanning confocal microscopy. Note that *(S)*-ene failed to cause receptor internalization unlike S1P, FTY720-P, or *(R)*-ene, which caused translocation of the $S1P_1$-eGFP construct from the plasma membrane to the cytoplasm. Calibration bar is 10 μm.

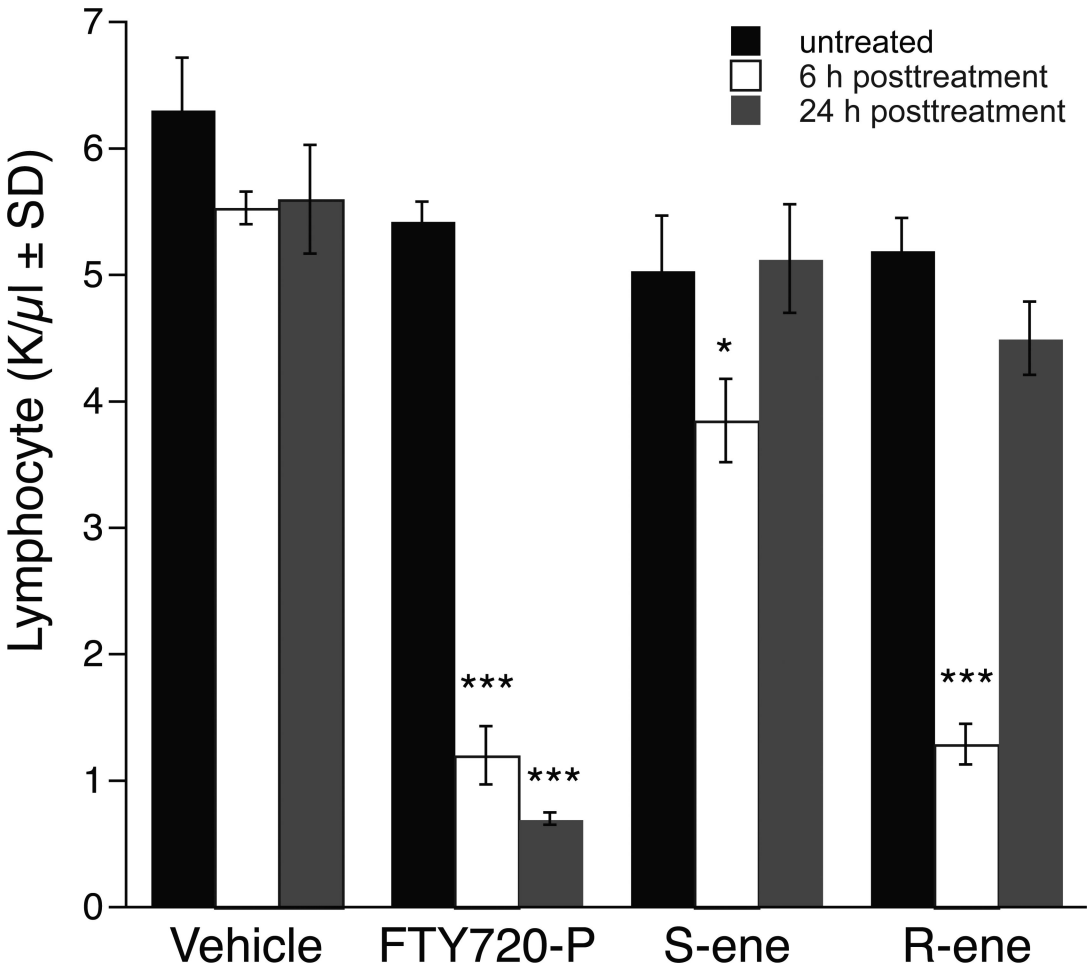

Fig. 6.

FTY720-P and *(R)*- or *(S)*-*ene* cause peripheral lymphopenia in C57BL/6 mice after 6 h of treatment. Mice received 1mg/kg of FTY720-P, *(R)*- or *(S)*-FTY720-vinylphosphonate, or vehicle (5% hydroxypropyl-β-cyclodextrin) via intraperitoneal injection. Blood was collected before treatment and 6 h and 24 h after injection, and peripheral circulating lymphocyte counts were determined. Note that unlike the durable lymphopenia in mice injected with FTY720-P, mice injected with *(R)*-ene or *(S)*-ene show no significant decrease of circulating peripheral lymphocytes by 24 h after treatment. Data points represent the mean ± SD. *$p < 0.05$, ***$p < 0.001$ relative to pretreatment counts.

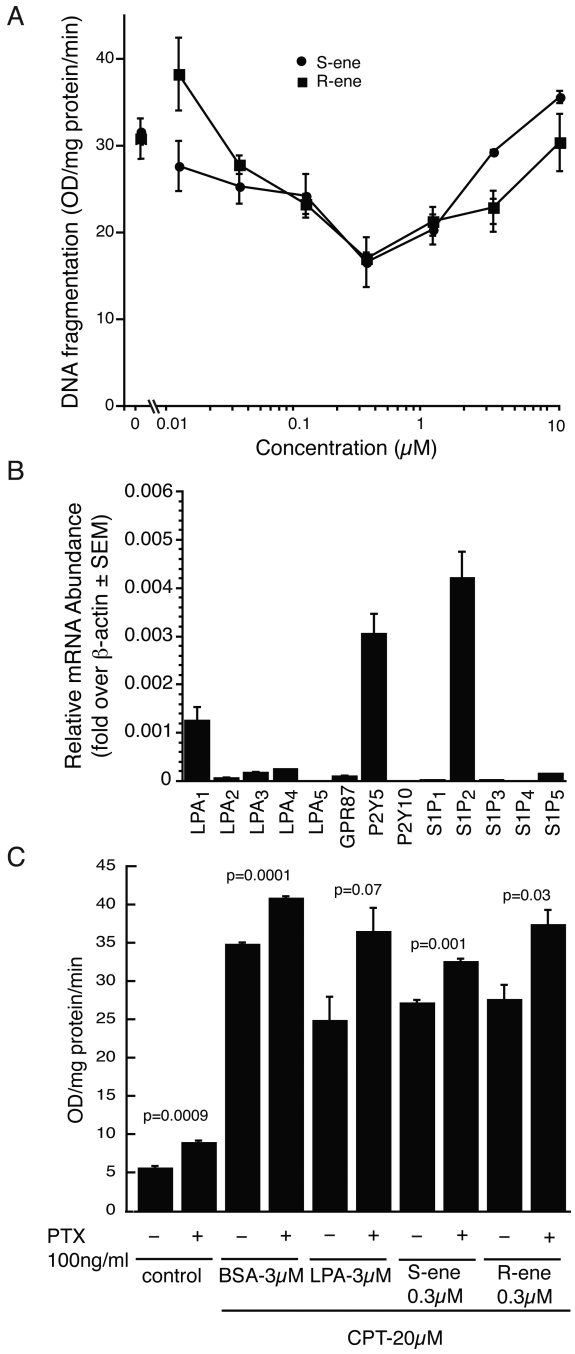

Fig. 7.

(R)- and *(S)*-FTY720-vinylphosphonates attenuate camptothecin-induced DNA fragmentation in IEC-6 cells, and relative abundance of LPA and S1P receptor transcripts in IEC-6 cells. (A) IEC-6 cells were pretreated with vehicle or compound for 15 min before treatment with camptothecin (20 μM) for 5 h. *(R)*-ene or *(S)*-ene dose-dependently attenuate camptothecin-induced DNA fragmentation. Both compounds showed the maximum protection at 300 nM but the effect diminished at higher concentrations. Data are the mean of three experiments ± SD. (B) Quantitative real-time PCR. Total RNA was extracted from IEC-6 cells and the expression level of each S1P or LPA receptor was determined. Expression levels were normalized to β-actin expression. Note that no detectable $S1P_1$

transcripts were found in the IEC-6 cells. (C) IEC-6 cells were incubated overnight in PTX (100 ng/ml), then pretreated with BSA, LPA, *(R)*-ene, or *(S)*-ene for 15 min before treatment with camptothecin (20 μM) for 5 h. Triplicate samples were analyzed; data are the mean ± SD.

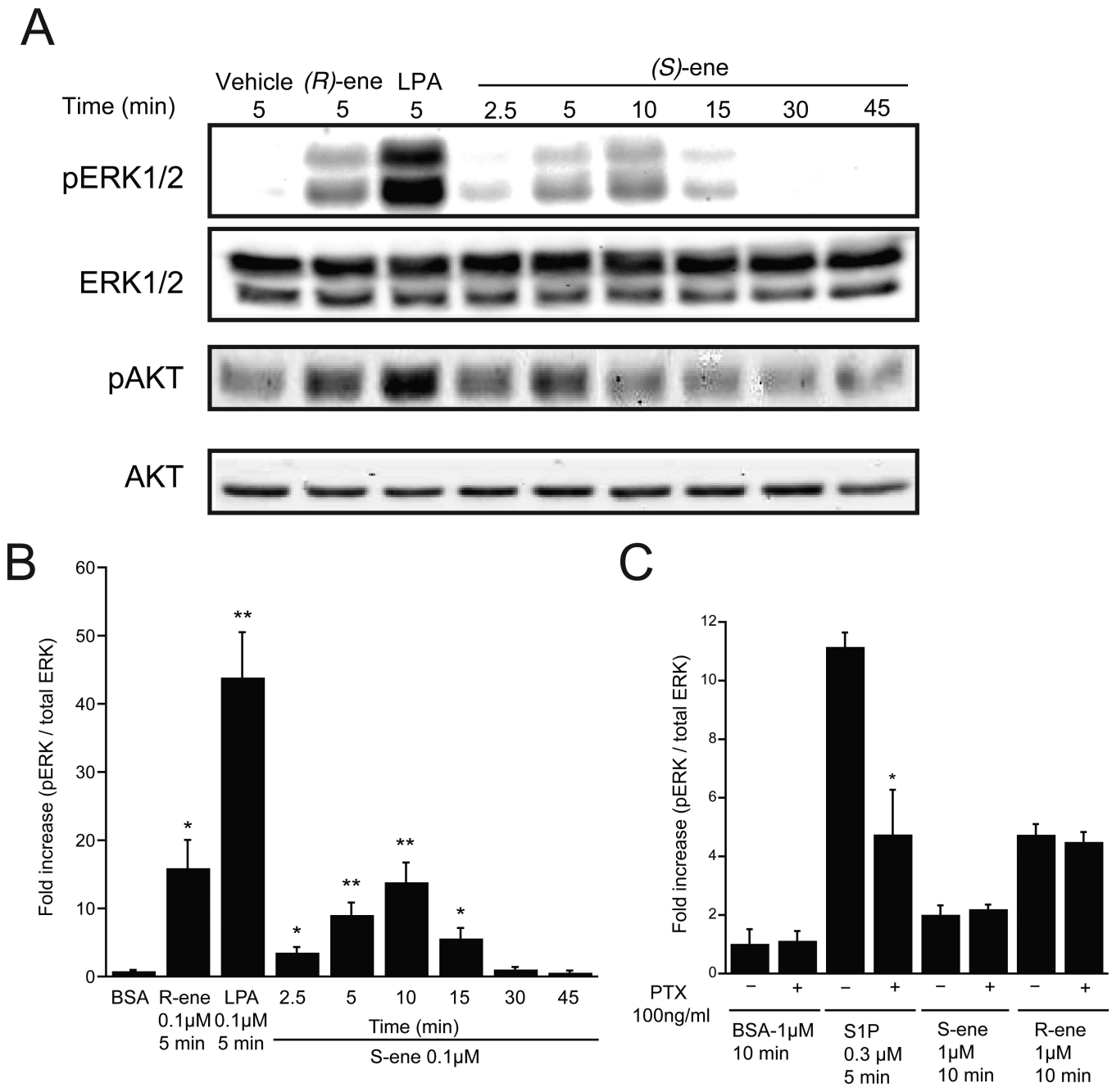

Fig. 8.

ERK1/2 and AKT activation in response to LPA, S1P, *(R)*- and *(S)-ene* in IEC-6 cells. (A) IEC-6 cells were exposed to 100 nM LPA or *(R)*-ene for 5 min, or 100 nM of *(S)*-ene for the time periods indicated and phosphorylated and total ERK1/2 (42 & 44 KDa) and AKT (60 KDa) were detected with appropriate antibodies. (B) The phospho-ERK1/2 and total ERK immunoblots shown in panel A were quantified by densitometry, and the results are expressed as the fold increase compared to control of the ratio of phospho-ERK to total ERK. (C) IEC-6 cells were incubated overnight in the presence of PTX (100 ng/mL) or vehicle, then incubated with S1P (300 nM) for 5 min, or else vehicle (BSA), *(S)*- or *(R)*-ene (1 μM) for 10 min. All samples were run in triplicate; data points represent the mean ± SD.

TABLE I

S1P receptor activation by FTY720-P and the phosphonate and vinylphosphonate analogues

Intracellular Ca^{2+} mobilization in response to S1P, FTY720-P, or analogues was measured in HTC4 cells expressing $S1P_{1\text{-}5}$ and CHO cells expressing P2Y10. The responses are reported in terms E_{max} (% of S1P maximal response) and EC_{50} (nM) ± standard deviation. Vector-transfected cells were not activated by any of the compounds. NA, not activated.

	$S1P_1$	**$S1P_2$**	**$S1P_3$**	**$S1P_4$**	**$S1P_5$**	**P2Y10**
Compound	**E_{max}, EC_{50}**	**E_{max}, EC_{50}**	**E_{max}, EC_{50}**	**E_{max}, EC_{50}**	**E_{max}, EC_{50}**	**E_{max}, EC_{50}**
S1P	100%, 4±1	100%, 47±2	100%, 12±1	100%, 6±2	100%, 2±1	100%, >500
FTY720-P	85%, 5±1	50%, >1000	23%, 63±34	41%, >500	NA	NA
(*R*)-vinyl-phosphonate	87%, 20±3	NA	13%, >500	NA	NA	NA
(*R*)-phosphonate	81%, 22±7	NA	13%, >300	NA	NA	NA
(*S*)-vinyl-phosphonate	NA	NA	NA	NA	NA	NA
(*S*)-phosphonate	57%, 71±38	NA	NA	NA	NA	NA

TABLE II

S1P receptor antagonism by (*S*)-FTY720-vinylphosphonate

Intracellular Ca^{2+} mobilization in response to S1P was measured in HTC4 cells expressing $S1P_{1\text{-}5}$ or CHO cells expressing P2Y10/ $G\alpha_{16}$. Cells were cotreated with S1P at the indicated concentrations and increasing concentrations of (*S*)-ene-phosphonate, and the inhibitory effects of (*S*)-ene-phosphonate on Ca^{2+} mobilization were determined. The responses were calculated in terms Ki ± standard deviation or maximal % inhibition of the measured S1P response.

Compound	$S1P_1$	$S1P_2$	$S1P_3$	$S1P_4$	$S1P_5$	P2Y10
(*S*)-vinylphosphonate	Ki = 384±59 nM (3 nM S1P)	40.0% inhibition at 30 mM (30 nM S1P)	Ki = 39±8 nM (10 nM S1P)	Ki = 1190±558 nM (5 nM S1P)	60.0% inhibition at 30 mM (30 nM S1P)	No inhibition at 30 mM (300 nM S1P)